https://doi.org/10.1016/j.scriptamat.2020.113693

Grain boundary-mediated plasticity accommodating the cracking process in nanograined gold: In situ observations and simulations

Xu-Sheng Yang[a, b*], Shuqing Yuan[a], Hui Fu[a], and Yun-Jiang Wang[c**]

[a]*State Key Laboratory of Ultra-precision Machining Technology, Department of Industrial and Systems Engineering, The Hong Kong Polytechnic University, Hung Hom, Kowloon, Hong Kong, China (E-mail: xsyang@polyu.edu.hk)*

[b]*Hong Kong Polytechnic University Shenzhen Research Institute, Shenzhen, China*

[c]*State Key Laboratory of Nonlinear Mechanics, Institute of Mechanics, Chinese Academy of Sciences, Beijing 100080, China (E-mail: yjwang@imech.ac.cn)*

In this study, the underlying atomic-scale plastic deformation mechanisms responsible for the crack propagation process in nanograined gold thin film with an average grain size of ~10 nm (ranging from ~2 nm to ~20 nm) is investigated by the in situ high-resolution transmission electron microscope observations (i.e., a homemade device with atomic force microscope inside transmission electron microscope) and atomistic molecular dynamic simulations. The real-time results based on the experimental observations and simulations uncover consistently that the crack propagation in nanograined gold thin film is accommodated by the grain boundary-mediated plasticity, which may result in the grain coalescence between neighboring nanograins. Furthermore, we find that the grain boundary-mediated plasticity is grain size-dependent, i.e., GB dislocation activities-induced grain rotation in relative larger grains and GB migration in relative smaller grains in comparison with a critical grain size of ~ 10 nm.

Keywords: Nanocrystalline metal; Crack propagation; Plastic deformation, In situ transmission electron microscope; Molecular dynamic simulations

* Corresponding author. xsyang@polyu.edu.hk (X.-S Yang). Tel: +852-27666604
** Corresponding author. yjwang@imech.ac.cn (Y.-J Wang). Tel: +86-10-82543931

Enhancing the mechanical properties and understanding the underlying plastic deformation mechanisms of metals have been the long-term objectives of materials scientists and engineers. The strength of the coarse-grained (CG) metals are mainly controlled by the interactions of intra-grain dislocations with grain boundaries (GBs) [1, 2] and/or other barriers [3]. In contrast, these dislocation activities are severely suppressed by the significantly refined grains and increased GB fraction in the nanogained (NG) metals with grain sizes down to nanometer scale (d < 100 nm), thus leading to the unusual high strength but poor ductility [4, 5]. Noticeably, the GB-mediated plasticity might take the place of the ordinary dislocation plasticity to dominate the softening deformation process of NG metals with grain size below a critical value (e.g., d < ~ 15-30 nm) [6-10].

Over the past decades, some advanced techniques, such as in situ transmission electron microscopy (TEM) observations and molecular dynamic (MD) simulations, have been widely developed to capture and visualize the dynamic information about the microstructural evolution during the plastic deformation/cracking process in NG metals. In this regard, most of the in situ observations and simulations revealed that the GB-mediated plasticity also dominate the potential nucleation and growth of nanovoids/nanocracks at GBs for coalescing the main cracks, leading to the intergranular cracking process in NG metals with grain sizes below certain critical values [11, 12]. Noticeably, various GB-mediated plasticity mechanisms, such as GB dislocations [13, 14], GB migration/sliding [15], and GB diffusion [16], etc., have been reported to be able to accommodate the cracking process of NG metals, suggesting a characteristic of size-dependence. To name a few, the crack propagation by purely atomic migration with steps at GB from the tip region to the crack rear was reported during the in situ TEM straining crack propagation process of NG gold (Au) thin film (d~ 10 nm) [17]. While some other in situ TEM experiments and MD

simulations of NG Au metals with comparable grain size reported the mechanism of grain rotation near the crack tip to accommodates their crack propagation processes [13-16]. In addition, even the grain rotation process might also be grain size-dependent, e.g., accomplished by cross-grain dislocation activities in larger grains (d > 6 nm) while GB dislocation activities in smaller grains (d < 6 nm) in NG Pt [14]. The discrepancy in size-dependent GB-mediated plasticity mechanisms might also be attributed to the complications associated with the nature of materials, e.g., loading condition and stress field near the crack tip during the cracking process. Nonetheless, the above description indicates that the GB-mediated plasticity mechanisms responsible for the crack propagation process of NG metals have not been well understood yet, meaning that more direct and detailed evidence is still needed.

Herein, we develop a homemade in situ TEM observation device (i.e., atomic force microscope (AFM) inside TEM) and MD simulations to uncover the underlying plastic deformation mechanisms responsible for the dynamic cracking process in NG Au thin film. As for the design of the homemade in situ AFM-TEM experiments, the sharp copper wire with a diameter of 0.5 mm and a length of 10 mm was first put into a Gold Coater (Scancoat Six, Edwards) as a substrate to sputter Au for ~15 seconds, as shown in Fig. 1(a). The TEM image in Fig. 1(b) shows that a ~200 nm-thick Au thin film has been successfully sputtered on the surface of copper wire. According to the contrast of the TEM image, a dash white line is added to separate the TEM image into two regions in Fig. 1(b). The right surface thinner region with clear GBs should be the pure Au thin film, which is also approved by the corresponding SAED pattern in Figure 1(c). The grain size statistical distribution in Fig. 1 (d) shows the grain size ranges from ~2 to ~22 nm of the sputtered NG Au thin film, denoting an average grain size of ~10 nm. In addition, Fig. 1 (e-f) show respectively a typical HRTEM image and inverse fast Fourier transfer (IFFT) image taken from

the rectangle frame in Fig. 1 (e), where the interplanar spacing is well characterized for the Au crystal. Noticeably, the TEM image of Fig. 1 (b) shows apparently that the surface of the sputtered NG Au thin film is not smooth with some grains protruded from the surface, possessing many nanocracks tips on the surface, as indicated by the dash red line in Fig. 1 (b). The copper wire with sputtered NG Au thin film was then installed on an in situ AFM-TEM holder (Nanofactory). The AFM tip is manipulated by a piezo-driven head and thus can be driven flexibly toward the protruding NG Au part, along the direction indicated by the arrows in Fig. 1 (b). Once the AFM tip is contacted to the surface of the protruding NG Au thin film, they will stick together easily due to the nanoscale adhesion effect. In addition, some grains on the surface of the NG Au thin film might even be worn off and attached to the AFM tip after the thin film is against by the AFM tip [18, 19]. Nonetheless, the adhesion effect between the AFM tip and NG Au thin film will not be weakened in the follow-up experiments. Instead, it might be enhanced because re-joining between these small grains would take place, which can also be understood by the cold-welding effect of the ultrathin metals at the nanoscale [20]. As a result, the propagation of these nanocracks can be induced and observed in NG Au thin film based on the design in our experiments. The real-time dynamic cracking process was observed by HRTEM (JEOL 2010F) operating at the voltage of 200 kV. Note that the substrate copper wire with excellent thermal conductivity could promptly release any potential thermal energy induced by the electron beam, thus maintaining the desired room temperature in NG Au thin film during the in situ AFM-TEM observations process.

The in situ AFM-TEM observation was first performed at a location away from the crack tip during the cracking process of the NG Au thin film. Fig. 2 shows a sequence of HRTEM images taken at different durations during the cracking process, demonstrating the GB migration-induced grain coalescence from two neighboring small grains with grain sizes below ~10 nm

(Supplementary Movie S1). Fig. 2(a) is the HRTEM image captured at the initial stage of cracking process, where two nanograins with grain sizes of ~8 nm and ~5 nm are marked as "G1" and "G2", respectively. Fig. 2(d) gives the schematic and corresponding IFFT patterns/images of initial grains G1 and G2 taken from the rectangle frames 1 and 2, respectively. Noticeably, the $(111)_{Au}$ planes with a interplanar spacing of ~0.229 nm can be easily indexed for the grain G1 in Figure 2(d1), while the live FFT pattern in Fig. 2(d2) indicates that the grain G2 does not exist any obvious crystallographic orientation under the same electron beam projection direction. Therefore, it can be concluded that initial grains G1 and G2 have different crystallographic orientations. Once the cracking process is in progress, the GB between grains G1 and G2 is moved toward the interior of G2, as proven by the HRTEM image in Fig. 2(b) and corresponding FFT patterns in Fig. 2(e), respectively. This cracking process is governed by the GB migration process and no obvious dislocation activities are found according to our observations. The GB migration process makes the crystallographic orientation of the migrated part in grain G2 rotate to the same as that of grain G1. As a result, it leads to an increase in the grain size of G1 while a decrease in the grain size of G2. As the cracking process continues, the GB migration process is continuously toward the interior of grain G2. At last, the HRTEM image in Fig. 2(c) and corresponding FFT patterns/images in Fig. 2(f) show that the crystallographic orientation of the whole grain G2 is rotated to the grain G1, resulting in the grain coalescence from these two neighboring grains.

Fig. 3 presents a series of HRTEM images taken at different durations to depict the microstructural evolution at one particular crack tip during the cracking process of NG Au thin film (Supplementary Movie S2), showing the crack blunting from ~110^{o} to ~135^{o}. In addition to the pure GB migration between small grains in Fig. 2 (grain sizes below ~10 nm), here we in situ observe another GB-mediated plasticity mechanism, i.e., grain rotation between relatively large

grains. Fig. 3(a) is the HRTEM image for the initial status at the crack tip, in which five nanograins are marked as “G1”, “G2”, “G3”, “G4” and “G5”, respectively. The grain sizes of G1 and G5 are over 20 nm, obviously larger than those of G2, G3, and G4 (approximately 10 nm or slightly below 10 nm). Initially, grains G2, G4, and G5 do not show any obvious crystallographic orientations under the current projection zone, as evidenced by corresponding live FFT patterns in Fig. 3(e). Fig. 3 (f-g) are respectively the IFFT images enlarged from the rectangle frames (f-g) in Fig. 3(a), in contrast, presenting the (111)Au planes for both grains G1 and G3. Noticeably, these two grains have a misorientation of ~11^{o} and an array of dislocations can be observed at the GB, as marked as “T” in Fig. 3(g). Once the crack blunting process is triggered, we first observe the slight GB migration between grains G1 and G2, i.e., the GB moves from the larger grain G1 toward the smaller grain G2, as shown in Fig. 3(b) and corresponding schematic in Fig. 3(k). However, this GB migration process is postponed with the crack blunting continues. Alternatively, the orientation of the region near the GB between grains G1 and G2 become to rotate, as highlighted blue line in Fig. 3(c) and region in Fig. 3(l), respectively, inducing a misorientation of ~17^{o} between the grain G1 and the rotated region in grain G2. Finally, Fig. 3(d) shows that the whole grain G2 is rotated to have a misorientation of ~17^{o} to grain G1, as evidenced by the IFFT image in Fig. 3(h) taken at the rectangle frame (h) in Fig. 3(d). In addition, it is noted that the GB migration also happens between two small grains, i.e., from grains G3 to G4 as schematically indicated in Fig. 3(l), leading to the grain coalescence from grains G3 and G4. As a result, a new coalescing grain G3 with grain size over 10 nm is then rotated to reduce the misorientation between grain G1 and G3 from ~11^{o} to ~8^{o}, which is evidenced by the IFFT image in Fig. 3(i) taken at the rectangle frame (i) in Fig. 3(d). In addition to the arrays of dislocations at the GB for accomplishing the small-angle tilt GBs between nanograins, as indexed in Fig. 3(g-i), GB dislocation activities can also be observed

according to the distortion regions near the GBs. Fig. 3(m) demonstrates schematically the final status of microstructure at the crack tip during the cracking process of NG Au thin film. In situ results in our work clearly indicate that the GB-mediated plasticity mechanism is grain size-dependent to accommodate the cracking process of NG Au thin film, i.e., GB activates-induced grain rotation in relative larger grains with grain sizes over ~10 nm, while the GB migration process in relative smaller grains with grain sizes below ~10 nm.

In addition to the in situ HRTEM observations, atomistic MD simulations were also performed to carry out the cracking process of NG Au thin film and uncover the corresponding plastic deformation mechanisms. The LAMMPS code [21] and embedded-atom method potential [22] were employed to build up a fully dense three-dimensional $70 \times 70 \times 20$ nm^3 NG Au model, which contains 100 Voronoi tessellation grains with grain size ranging from ~5 nm to ~20 nm, denoting an average grain size of ~10 nm. The relaxation at 500 K for 1 ns was conducted to initially stabilize the model, especially the GB atoms, within a Nosé-Hoover thermostat [23, 24]. Then, a surficial crack tip with a length of 23 nm and a width of 2 nm was introduced in the middle of the simulated sample, as shown in Fig. 4(a1). The mechanical loading perpendicular to the crack length direction was imposed with a constant strain rate of 2×10^8 s^{-1} to generate the crack blunting, i.e., mimic a model I crack system. During the crack blunting, lattice defects were recognized by the common neighbor analysis (CNA) [25]. Note that both of GB migration and grain rotation would lead to the grain coalescence with the change of orientations. Fig. 4 (a1-c1) shows that a vertical straight line with 1 nm width (> -60, < -50 Å) is selected to trace the evolution of grain orientations during the cracking process. The change of orientation happens if the line is not straight anymore, potentially suggesting the GB-mediated plasticity via GB migration and/or grain rotation. Fig. 4 (b1-c1) are the images at the strain levels of 8.8%, and 30%, respectively, indicating

the possible occurrence of grain rotation and/or GB migration as the vertical straight line is gradually not straight anymore. Interestingly, the dislocation behavior visualized by Dislocation Extraction Algorithm (DXA) in Fig. 4(a2-c2) and atomic-scale stress distribution calculated by Viral theorem in Fig. 4(a3-c3) consistently show that some dislocation activities with stress concertation mainly at GBs to accommodate the cracking process. It means that the dislocation behaviors also operate in extremely small grains and may facilitate GB plasticity within the confined volumes.

More specifically, Fig. 5(a-c) gives a series of simulated atomic images at the crack tip to reveal the corresponding deformation mechanisms. Initially, four nanograins with different grain sizes and orientations are marked in Fig. 5(a) as “G1”, “G2”, “G3”, and “G4”, respectively. With the cracking process in progress, on one hand, the grain rotation happens between two large grains G1 and G2. As indicated in Fig. 5(a-b), the misorientation between them is gradually reduced from ~ 13^{o} to ~8^{o}, by rotating the orientation of grain G2. On the other hand, the GB migration process happens in small grains, i.e., GB is migrated from grains G2 and G4 toward the grain G3. Finally, Fig. 5(c) shows that both grain rotation and GB migration processes lead to the grain coalescence between two neighboring grains, forming two new coalescing grains G1 and G4. Furthermore, Fig. 5(a-b) indicates that the grain rotation should be accomplished by the GB dislocation activities, which is also suggested by the increased dislocation density in Fig. 5(d). One might note that the external loading directions between experiments and simulations are different in this study. However, the localized nanocrack tips on the surface of the protruding NG Au thin film have various orientations, which make some particular crack tips have the same cracking mode as that in simulations, as shown in Fig. 3 and Fig. 4-5.

Although several types of GB-mediated plastic mechanisms have been explored in various NG metals, such as Ni[26], Al[27], Pt[14], Cu[28] and Au[15, 29, 30], etc., there is still limited direct experimental evidence for the cracking process, especially involving the grain size-dependence in the NG metals with grain sizes below ~ 20 nm. In this study, the direct evidence for the grain size-dependent GB-mediated cracking mechanisms by in situ HRTEM observations and simulations are consistent. Grain rotation is one well-known characteristic responsible for the plasticity of polycrystalline materials. However, the traditional grain rotation, which is accomplished by cross-grain gliding of numerous dislocations to reorient one entire grain, is expected to subside in NG metals with such extremely tiny grains at room temperature, especially below certain critical values. Alternatively, a particular GB mediated-plasticity, i.e., GB dislocation activities-induced grain rotation with the climb of dislocations at GBs, would dominate the plastic deformation process [14, 31], as observed in some grains (e.g., ~10 nm < d < ~20 nm) during the cracking process in this work. GB migration is another prevalent GB mediated-plastic deformation mode in NG metals. Note that GB migration mechanisms in NG metals would be influenced by several factors, e.g., GB size and structure, loading condition, and temperature. Therefore, numerous theoretical and experimental investigations have been conducted to propose various GB migration mechanisms, such as GB diffusion [15, 26], atomic shuffling [32], and shear-coupled migration [29, 30], etc. For instance, the shear-coupled migration of $\sum 11(113)$ coherent GBs in Au bicrystals was revealed to be realized by GB disconnections and/or GB dislocations [29]. In the present work, however, no obvious dislocation activities are observed during the GB migration responsible for the cracking process of the small grains (< ~10 nm) in NG Au thin film. In addition to some pre-existing defects (e.g., solutes, vacancies, dislocations, stacking faults, and/or twins) at the GBs, increasing the GB diffusion coefficient could also substantially promote

the GB mobility, which is beneficial to the GB migration. Noticeably, the GB diffusion coefficient in NG metals could be ~2-3 orders of magnitude larger than that in CG counterparts [33-36]. Therefore, the observed GB migration in small grains with grain size below ~ 10 nm is expected to be able to accommodate the strain rate generated in our experiments. As a result, our in situ experiments and simulations uncover consistently the size-dependent GB plasticity, GB dislocation activities-induced grain rotation in large grains (d > ~10 nm) and GB migration in small grains (d < ~10 nm), result in the grain coalescence to accommodate the crack propagation in NG Au thin film. In addition, it should be noticed that the GB-mediated plasticity of the sputtered NG Au thin film under in situ AFM-TEM loading in our work might not be able to fully represent that of some other common bulk counterparts. This because some critical factors such as the processing routine, loading conditions, and the specimen geometry are different between them. Nonetheless, our homemade in situ TEM device with the facile procedure of nanofabrication, and mechanical loading, and observation would provide opportunities to systematically investigate the mechanical failures and underlying plastic deformation mechanisms of some nanoscale components and/or devices.

This work was supported by the National Natural Science Foundation of China Projects (Nos. 51701171 and 51971187) and the PolyU project (No. G-YBZ3). YJW was supported by the NSCF (Nos. 11672299 and 12072344), the National Key Research and Development Program of China (No. 2017YFB0701502), and the Youth Innovation Promotion Association of Chinese Academy of Sciences (No. 2017025).

References:

[1] E.O. Hall, Proc. Phys. Soc., B 64(9) (1951) 747.

[2] N.J. Petch, J. Iron and Steel Institute 174 (1953) 25-27.

[3] J.P. Hirth, J. Lothe, Theory of Dislocations, John Wiley and Sons1982.

[4] M.A. Meyers, A. Mishra, D.J. Benson, Prog. Materi. Sci. 51(4) (2006) 427-556.

[5] S. Yip, Nature 391(6667) (1998) 532-533.

[6] J. Schiotz, F.D. Di Tolla, K.W. Jacobsen, Nature 391(6667) (1998) 561-563.

[7] H.V. Swygenhoven, Science 296(5565) (2002) 66-67.

[8] L. Lu, X. Chen, X. Huang, K. Lu, Science 323(5914) (2009) 607-610.

[9] J. Schiotz, K.W. Jacobsen, Science 301(5638) (2003) 1357-1359.

[10] X. Li, Y. Wei, L. Lu, K. Lu, H. Gao, Nature 464(7290) (2010) 877-880.

[11] D. Farkas, S. Van Petegem, P.M. Derlet, H. Van Swygenhoven, Acta Mater. 53(11) (2005) 3115-3123.

[12] D. Farkas, H. Van Swygenhoven, P.M. Derlet, Phys. Rev. B 66(6) (2002) 060101.

[13] E. Hosseinian, S. Gupta, O.N. Pierron, M. Legros, Acta Mater. 143 (2018) 77-87.

[14] L. Wang, J. Teng, P. Liu, A. Hirata, E. Ma, Z. Zhang, M. Chen, X. Han, Nat. Commun. 5(1) (2014) 4402.

[15] L. Wang, T. Xin, D. Kong, X. Shu, Y. Chen, H. Zhou, J. Teng, Z. Zhang, J. Zou, X. Han, Scr. Mater. 134 (2017) 95-99.

[16] S. Kumar, X. Li, A. Haque, H. Gao, Nano Lett. 11(6) (2011) 2510-2516.

[17] H. Wang, A. Nie, J. Liu, P. Wang, W. Yang, B. Chen, H. Liu, M. Fu, Scr. Mater. 65(5) (2011) 377-379.

[18] G. Wang, J. Lian, T.-Y. Zhang, RSC Adv. 3(46) (2013) 24017-24020.

[19] G. Wang, J. Lian, Q. Jiang, S. Sun, T.-Y. Zhang, J. Appl. Phys. 116(10) (2014) 103518.

[20] Y. Lu, J.Y. Huang, C. Wang, S. Sun, J. Lou, Nat. Nanotechnol. 5(3) (2010) 218-224.

[21] S. Plimpton, J. Compu. Phys. 117(1) (1995) 1-19.

[22] Y. Mishin, M.J. Mehl, D.A. Papaconstantopoulos, A.F. Voter, J.D. Kress, Phys. Rev. B 63(22) (2001) 224106.

[23] S. Nosé, Mole. Phys. 52(2) (1984) 255-268.

[24] W.G. Hoover, Phys. Rev. A 31(3) (1985) 1695-1697.

[25] J.D. Honeycutt, H.C. Andersen, J. Phys. Chem. 91(19) (1987) 4950-4963.

[26] Z. Shan, E.A. Stach, J.M.K. Wiezorek, J.A. Knapp, D.M. Follstaedt, S.X. Mao, Science 305(5684) (2004) 654-657.

[27] Z. Shan, J.M.K. Wiezorek, J.A. Knapp, D.M. Follstaedt, E.A. Stach, S.X. Mao, Appl. Phys. Lett. 92(9) (2008) 091917.

[28] Q. Li, L. Wang, J. Teng, X. Pang, X. Han, J. Zou, Scr. Mater. 180 (2020) 97-102.

[29] Q. Zhu, G. Cao, J. Wang, C. Deng, J. Li, Z. Zhang, S.X. Mao, Nat. Commun. 10(1) (2019) 156.

[30] Q. Zhu, S.C. Zhao, C. Deng, X.H. An, K.X. Song, S.X. Mao, J.W. Wang, Acta Mater. 199 (2020) 42-52.

[31] P. Liu, S.C. Mao, L.H. Wang, X.D. Han, Z. Zhang, Scr. Mater. 64(4) (2011) 343-346.

[32] K.L. Merkle, L.J. Thompson, F. Phillipp, Phys. Rev. Lett. 88(22) (2002) 225501.

[33] X.-S. Yang, Y.-J. Wang, H.-R. Zhai, G.-Y. Wang, Y.-J. Su, L.H. Dai, S. Ogata, T.-Y. Zhang, J. Mech. Phys. Solids 94 (2016) 191-206.

[34] C. Herzig, S.V. Divinski, Mater. Trans. 44(1) (2003) 14-27.

[35] R. Würschum, S. Herth, U. Brossmann, Adv. Eng. Mater. 5(5) (2003) 365-372.

[36] Y.-J. Wang, G.-J.J. Gao, S. Ogata, Phys. Rev. B 88(11) (2013) 115413.

Figure 1

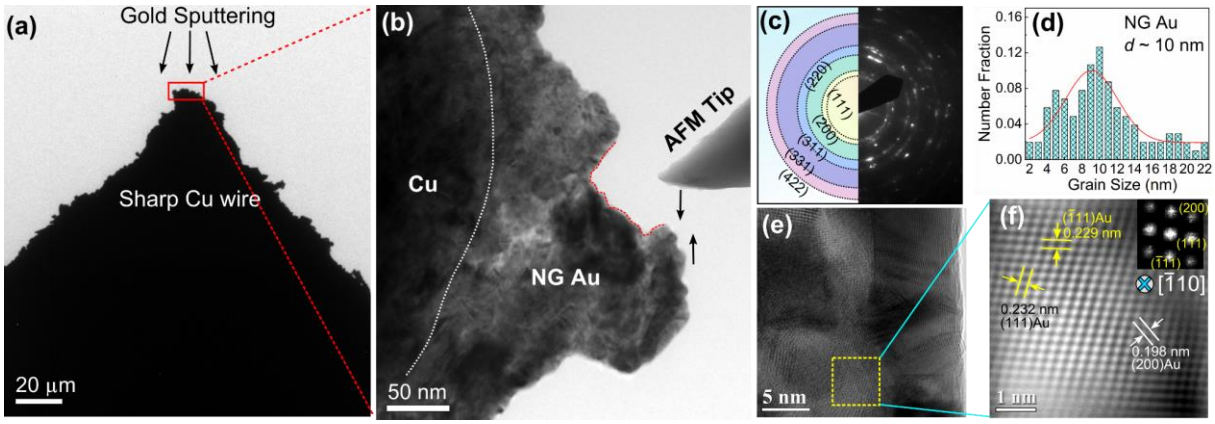

Figure 1 | The homemade in-situ AFM-TEM for observing the cracking process of NG Au thin film. (a) TEM image showing that Au thin film is sputtered on the sharp Cu wire tip by a Gold Coater. (b) The TEM image showing the sputtered Au thin film is NG structure with nanocracks pre-existing on the surface (as indicated by the dash red line). These pre-existed nanocracks would be propagated when the NG Au thin film is moved to against the AFM tip along the direction indicated by the arrow. (c) SAED pattern of the right surface thinner region in (b) indicating the pure NG Au structure. (d) Grain size statistical distribution of NG Au thin film, denoting an average grain size of ~10 nm. (e) A HRTEM image and (f) corresponding atomic IFFT image taken from the rectangle frame in (e), showing the atomic structure of NG Au.

Figure 2

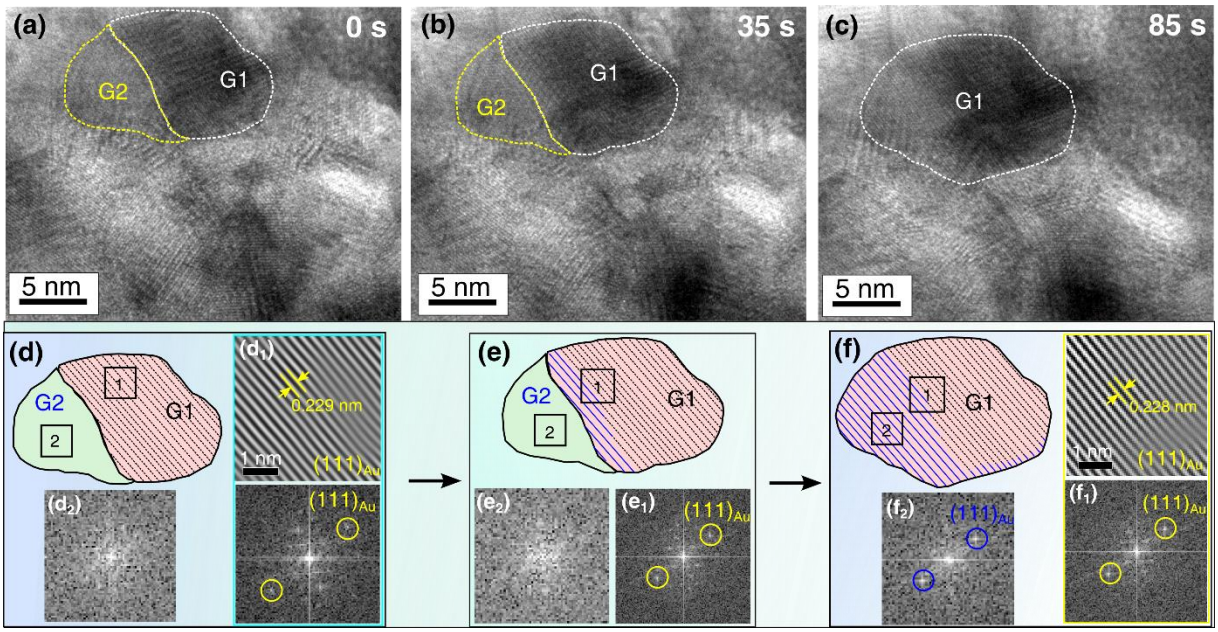

Figure 2 | In situ observation of the GB migration-induced grain coalescence during the cracking process. (a-c) A sequences of HRTEM images showing that the GB migration process induces the GB to move toward the interior of G2, resulting in the grain coalescence from G1 and G2. (d-f) The schematics, corresponding live FFT patterns and IFFT images taken from the rectangle frames 1 and 2, respectively, providing the details of the dynamic process of GB migration.

Figure 3

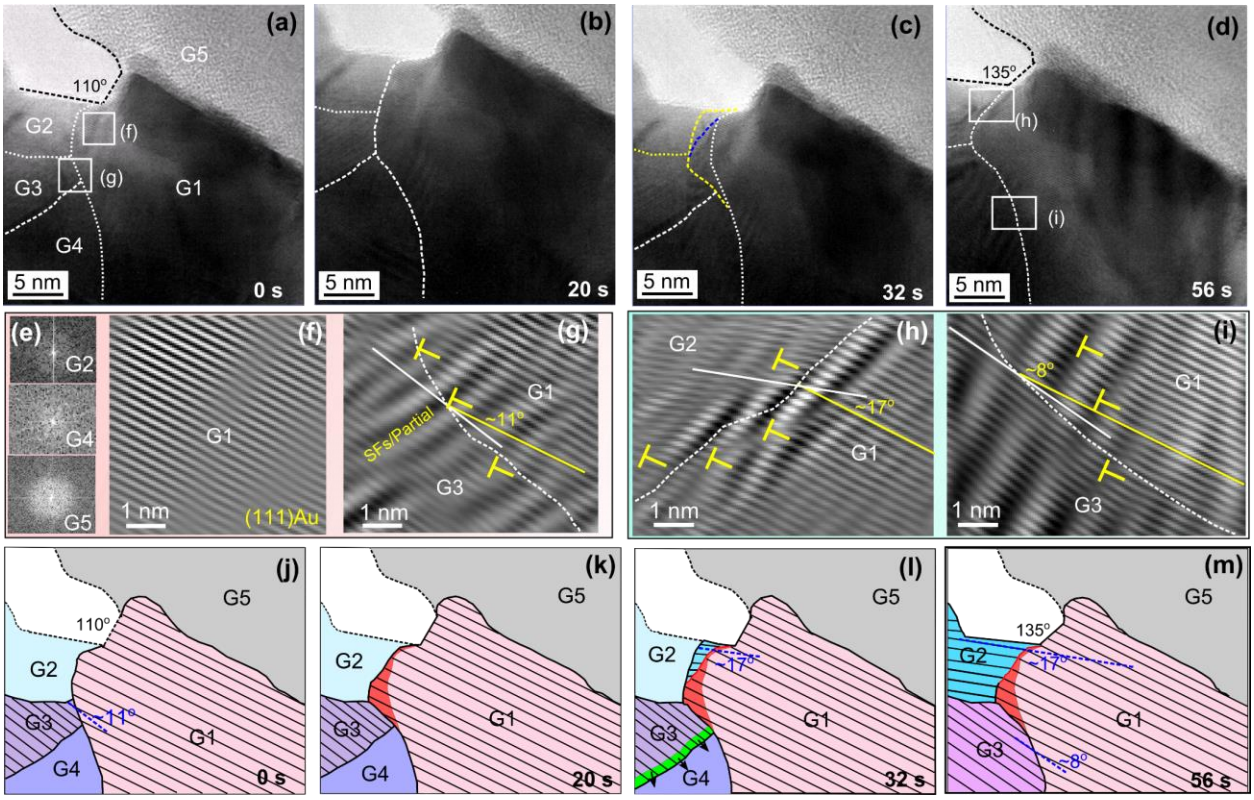

Figure 3 | In situ observation of the GB migration and grain rotation at the crack tip during the cracking process. (a-d) A sequences of HRTEM images showing the crack blunting from ~110^{o} to ~135^{o} at one typical crack tip. (e) The live FFT patterns of G2, G4, G5, and (f-g) IFFT images taken from the rectangle frames (f-g) in (a). (h-i) The IFFT images taken from the frames in (d). (j-m) Schematics showing the microstructural evolution during the crack blunting, which is accommodated by the GB migration and grain rotation.

Figure 4

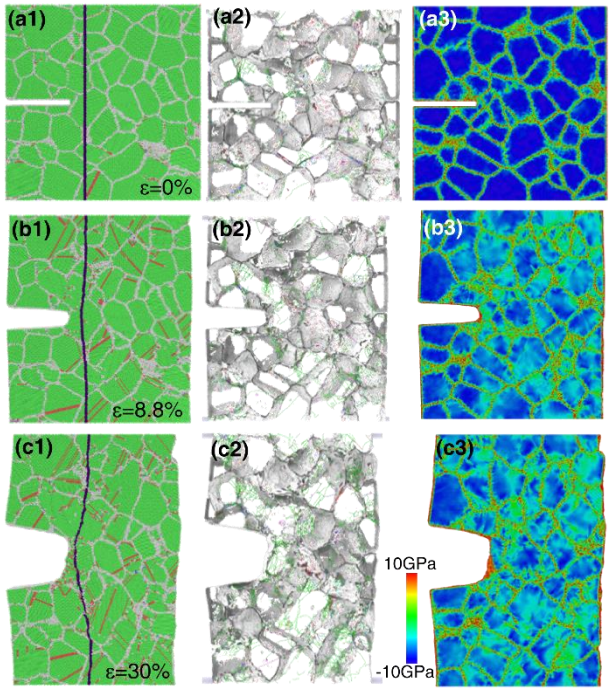

Figure 4 | MD simulation of the cracking process in NG Au. (a1-c1) The crack blunting process of NG Au at several representative strain levels of 0%, 8.8%, and 30%, respectively, showing the change of grain orientations as the marked vertical straight line is gradually not straight anymore. (a2-c2) The corresponding dislocation behaviors visualized by DXA, and (a3-c3) atomic-scale stress distribution calculated via Viral theorem showing the dislocation activities/stress are mainly concentrated at the GBs during the cracking process.

Figure 5

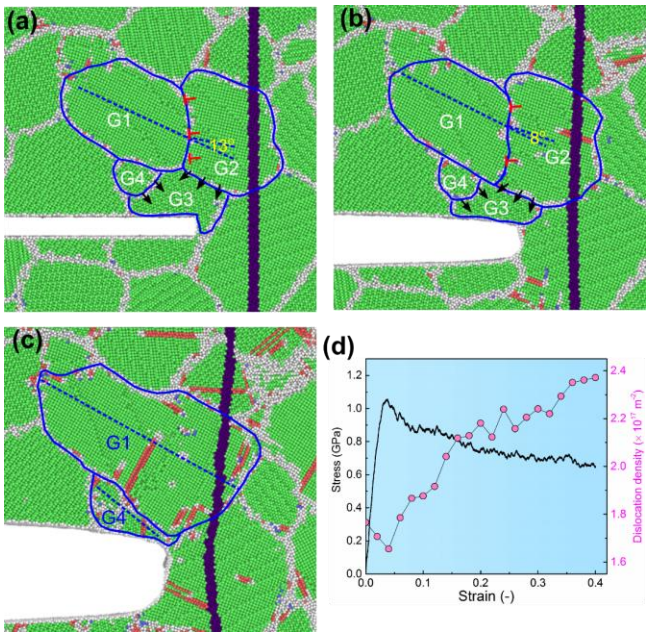

Figure 5 | MD simulation of GB migration and grain rotation at the crack tip during the cracking process. (a-c). A series of simulated images showing the GB migration and grain rotation, resulting in the grain coalescence from G1-G2 and G3-G4. (d) The stress-strain curve and corresponding evolution of the dislocation density during the cracking process.